

Article

Short-Circuit Fault Current Parameter Prediction Method Based on Ultra-Short-Time Data Window

Mengjiao Wang * , Xinlao Wei and Zhihang Zhao

Key Laboratory of Engineering Dielectrics and Its Application, Ministry of Education, School of Electrical and Electronics Engineering, Harbin University of Science and Technology, Harbin 150080, China

* Correspondence: wangmengjiao1102@163.com

Abstract: The prediction of short-circuit current parameters is essential for the adoption of short-circuit fault limiting techniques and the reliable cut-off of circuit breakers. In order to quickly and accurately predict the short-circuit current waveform parameters, a short-circuit fault current prediction method based on ultra-short-time data windows (UDWs) is proposed. First, a mathematical model for describing short-circuit faults is constructed and the characteristics of short-circuit currents are analyzed. Then, the principle of the UDW method for predicting short-circuit current waveform parameters is derived, the correctness of the principle is verified by setting-up an ideal signal through simulation, and the exponential and linear expressions fitted to the curve are analyzed and compared with the improved half-wave Fourier method for predicting current parameters. Finally, trend filtering technology is proposed to eliminate high-frequency interference and white noise interference. The results show that the ultra-short-time data window method can quickly and accurately predict the short-circuit current waveform parameters, where the exponential expression is a better fit to the waveform, and the trend filtering technique enables the elimination of high-frequency and white noise interference in the initial stages of prediction.

Keywords: ultra-short-time data windows; trend filtering technology; current amplitude; high-frequency interference; white noise interference



Citation: Wang, M.; Wei, X.; Zhao, Z. Short-Circuit Fault Current Parameter Prediction Method Based on Ultra-Short-Time Data Window. *Energies* **2022**, *15*, 8861. <https://doi.org/10.3390/en15238861>

Academic Editors: Seyed Morteza Alizadeh and Akhtar Kalam

Received: 21 October 2022

Accepted: 10 November 2022

Published: 23 November 2022

Publisher's Note: MDPI stays neutral with regard to jurisdictional claims in published maps and institutional affiliations.



Copyright: © 2022 by the authors. Licensee MDPI, Basel, Switzerland. This article is an open access article distributed under the terms and conditions of the Creative Commons Attribution (CC BY) license (<https://creativecommons.org/licenses/by/4.0/>).

1. Introduction

Of all electrical system accidents, short-circuit faults are the most serious in terms of damage. The energy released by the short-circuit arc and the electric power generated by the short-circuit current will cause serious damage to electrical equipment, even explosion or fire [1,2]. In addition, the increasing short-circuit current will lead to the short-circuit at the outlet near the transformer, causing the winding deformation of the main transformer and other faults, leaving the transformer in a sub-health operation state, laying a great hidden danger for the safe operation of the power grid [3,4]. At present, the main way to deal with short-circuit faults is to extract effective information from the transient process to achieve early diagnosis of short-circuit faults, and then take certain measures to limit them [5–7]. If the pattern of short-circuit current changes can be accurately predicted within the shortest possible time after the occurrence of a short-circuit fault, the correct technical measures against short-circuit faults can be taken precisely on the basis of such predictions and the capacity of the different types of anti-short-circuit fault measures already available in the system to obtain the best anti-short-circuit fault effect [8,9]. When a short-circuit fault occurs in the line, the current may rise dozens or even hundreds of times in a few milliseconds, seriously endangering system safety [10,11]. Therefore, how to quickly and accurately predict the short-circuit current waveform parameters after the occurrence of a short-circuit fault, and take the best anti-short-circuit fault measures to minimize the damage caused by short-circuit faults and ensure the safe and stable operation of the power system is of great importance [12–14]. However, there are often high-frequency

interference and white noise interference in the actual power system, which will have a greater impact on the accuracy of the prediction [15,16]. Therefore, it is necessary to fully consider these interfering factors, and strive for rapid identification while ensuring the accuracy of fault prediction.

The prediction of short-circuit current parameters is mainly focused on the prediction of the short-circuit current amplitude, while there is little literature on the identification of all parameters of the current waveform. In [17], a two-dimensional cloud model was used to predict the peak, but the two-dimensional cloud model is an uncertain prediction. Although the average relative error is low, the individual prediction error is greater than 5%, which is not conducive to practical application. In [18], the wavelet transform multi-resolution fast algorithm (MALLAT) was used, but this algorithm did not consider the attenuation of the DC component and the harmonic component of the current after the fault, and there will be a large deviation in the calculation of the linear relationship constant. In [19–21], neural network algorithms were used to predict peaks, but training required significant amounts of data, resulting in long training times and a tendency to fall into local optima. In [22,23], least squares was used to identify short-circuit current parameters, but this algorithm did not take into account the influence of harmonic factors, causing large errors in the waveform fitting process. In [24,25], the improved half-wave Fourier algorithm was used to fit the short-circuit current waveform, but the algorithm guarantees accuracy on the premise that the signal contains only odd harmonics, but when the content of even harmonics in the signal increases, the error in the algorithm's calculation results also increases significantly.

In order to meet the requirements of both speed and accuracy, this paper proposes a short-circuit fault current parameter prediction method based on ultra-short-time data windows (UDWs). First, a mathematical model describing the short-circuit fault is established in Section 2. In Section 3, the principle of the UDW method used to predict short-circuit current waveform parameters is described in detail. In this section, the exponential and linear expressions in the UDW method are compared by simulation and analyzed in comparison with the improved half-wave Fourier method. In Section 4, trend filtering technology is proposed to eliminate high-frequency interference and white noise interference. A single-phase small-capacity prototype model is used to simulate a single-phase short-circuit fault for experimental verification, and the test results are compared and analyzed with the simulation results to further validate the feasibility and accuracy of the proposed UDW prediction of short-circuit current parameters in Section 5. Finally, conclusions are summarized in Section 6.

The results show that the UDW method proposed in this paper can predict the short-circuit current waveform parameters quickly and accurately, and both the exponential and linear expressions fit well compared to the actual waveform, with the exponential expression fitting a curve closer to the actual curve. The proposed trend filtering technique can eliminate the high-frequency and white noise interference at the early stage of prediction.

2. Mathematical Model for Short-Circuit Fault

The most common short-circuit faults in transmission lines are single-phase ground short-circuit faults [26,27]. As shown in Figure 1, assuming that the supply voltage at t_0 ($t_0 = 0$) is used as the starting point for timing, the supply voltage can be set to $u_s = U_m \sin \omega t$. Assuming that the short-circuit impedance from the short-circuit point to the power supply is $R_s + j\omega L_s$ and the load impedance is $R_L + j\omega L_L$, and that a short-circuit fault occurs in the t_d system at some point after t_0 :

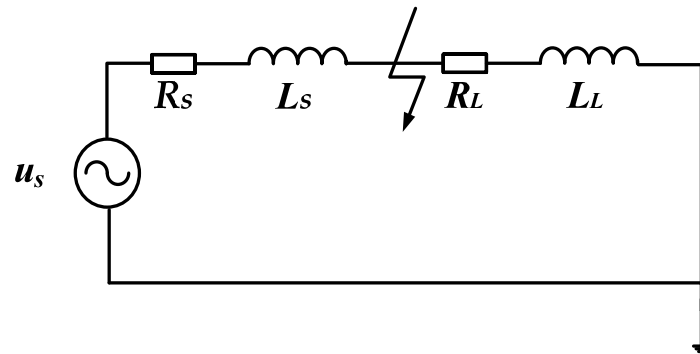


Figure 1. Basic model for single-phase earth short-circuit faults.

According to the basic principles of the circuit, from moment t_0 , the short-circuit current expression is

$$i_s(t) = I_{bm} \sin(\omega t - \varphi_1) + N_1 e^{-\alpha(t-t_d)} = I_{bm} \sin(\omega t - \varphi_1) + (i(t_d) - I_{bm} \sin(\omega t_d - \varphi_1)) e^{-\alpha(t-t_d)} \quad (1)$$

In Equation (1), I_{bm} is the amplitude of the steady-state component of the short-circuit current, $I_m = U_m / \sqrt{R_s^2 + (\omega L_s)^2}$. α is the short-circuit current transient component decay time constant, $\alpha = R_s / L_s$. φ_1 is the phase difference between the supply voltage and the steady-state component of the short-circuit current after a fault has occurred, $\varphi_1 = \arctg \omega L_s / R_s$. N_1 is starting value of the transient component, t_d is the moment of short-circuit, and $i(t_d)$ is the instantaneous value of the current at the moment of the short-circuit.

The short-circuit current can be divided into two parts: the steady-state component with sinusoidal changes and the attenuation transient component. The short-circuit current and bus voltage waveform are shown in Figure 2. It shows that after a short-circuit fault occurs, the current rises sharply.

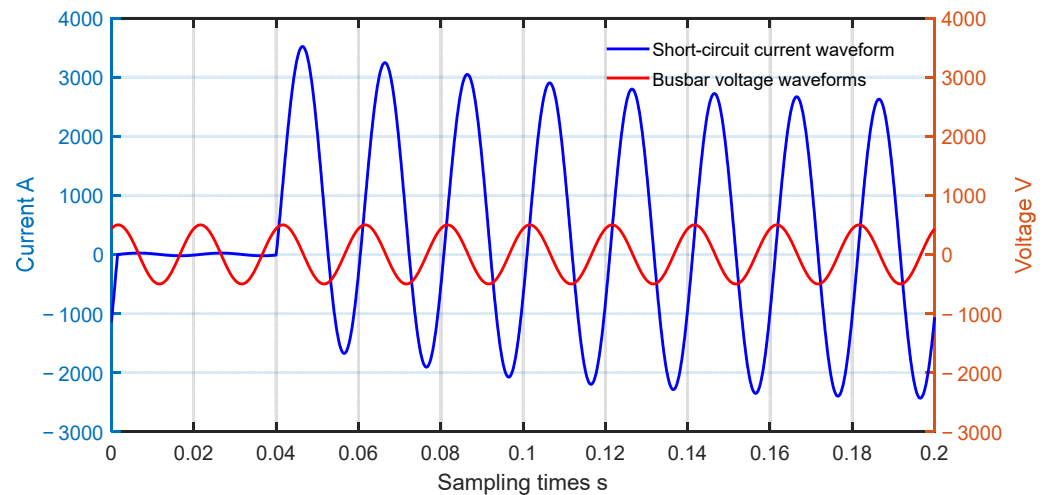


Figure 2. Voltage and current waveform.

3. Short-Circuit Current Waveform Parameters Prediction Based on UDW

The traditional least squares method for predicting short-circuit current parameters does not take into account the influence of harmonic factors and causes large errors, and the improved half-wave Fourier algorithm cannot accurately predict when the even harmonic content is too high. In response to these problems, this section presents a novel method for the prediction of short-circuit current waveform parameters, the Ultra-short-time Data Window (UDW) method. The principle of the UDW method for predicting short-circuit current waveform parameters is described in detail, and the predictive power of the two

expressions present during the fitting of the short-circuit current curve is compared by simulation. To further validate the accuracy of the method, the UDW method is compared with the improved half-wave Fourier method, which leads to the final conclusions.

3.1. Prediction Principles

In practical power systems, the statistically obtained short-circuit current transient component decays out in about 8 to 10 cycles, i.e., in the time range of (160 to 200) ms. Therefore, even within a relatively short time frame after the short-circuit fault occurs, it is unscientific not to consider the changes in the transient components of the short-circuit current at all [28]. However, if the problem is considered within a very short time frame after the occurrence of a short-circuit fault, the change in the short-circuit current transient component within this time frame is negligible. Thus, for a very short time after the occurrence of a short-circuit, the short-circuit current can be approximated as

$$\begin{aligned} i_s(t) &= I_{bm} \sin(\omega t - \varphi_1) + N_1 e^{-\alpha(t-t_d)} \\ &= I_{bm} \sin(\omega t - \varphi_1) + (I_0 - I_{bm} \sin(\omega t_d - \varphi_1)) e^{-\alpha(t-t_d)} \\ &= I_{bm} (\sin \omega t \cos \varphi_1 - \cos \omega t \sin \varphi_1) + (I_0 - I_{bm} (\sin \omega t_d \cos \varphi_1 - \cos \omega t_d \sin \varphi_1)) e^{-\alpha(t-t_d)} \\ &= X_1 \sin \omega t - X_2 \cos \omega t + (I_0 - X_1 \sin \omega t_d + X_2 \cos \omega t_d) e^{-\alpha(t-t_d)} \end{aligned} \quad (2)$$

In Equation (2), $X_1 = I_{bm} \cos \varphi_1$ and $X_2 = I_{bm} \sin \varphi_1$.

The variation in the transient component of the short-circuit current over an ultra-short period of time during the data window can be approximated by a linear expression. Therefore, in a short period of time after the short-circuit occurs, the short-circuit current can be approximated as

$$\begin{aligned} i_s(t) &= X_1 \sin \omega t - X_2 \cos \omega t + (I_0 - X_1 \sin \omega t_d + X_2 \cos \omega t_d) e^{-\alpha(t-t_d)} \\ &\approx X_1 \sin \omega t - X_2 \cos \omega t + (I_0 - X_1 \sin \omega t_d + X_2 \cos \omega t_d) (1 - \alpha(t-t_d)) \\ &= X_1 k_s(t) - X_2 k_c(t) + (I_0 - X_1 k_{sd} + X_2 k_{cd}) (1 - \alpha \Delta(t)) \\ &= X_1 k_s(t) - X_2 k_c(t) + (I_0 - X_1 k_{sd} + X_2 k_{cd}) - (I_0 - X_1 k_{sd} + X_2 k_{cd}) \alpha \Delta(t) \\ &= X_1 k_s(t) - X_2 k_c(t) + X_3 - X_4 \Delta(t) \end{aligned} \quad (3)$$

In Equation (3), $k_s(t) = \sin \omega t$, $k_c(t) = \cos \omega t$, $k_{sd} = \sin \omega t_d$, $k_{cd} = \cos \omega t_d$, $\Delta(t) = t - t_d$, $X_3 = (I_0 - X_1 k_{sd} + X_2 k_{cd})$, $X_4 = (I_0 - X_1 k_{sd} + X_2 k_{cd}) \alpha$, and $\alpha = X_4 / X_3$. Only X_1 , X_2 , X_3 , and X_4 are unknown quantities that can be found by sampling the values multiple times using the least squares method.

The relationship between X_1 , X_2 , X_3 , and X_4 and the parameters to be sought in the short-circuit current waveform are

$$\begin{cases} I_{bm} = \sqrt{X_1^2 + X_2^2} \\ \varphi_1 = \arctg(X_1/X_2) \\ \alpha = X_4/X_3 \end{cases} \quad (4)$$

From Equation (4), X_1 , X_2 , X_3 , and X_4 are obtained, and so are the parameters to be obtained for the short-circuit current waveform.

Assuming that the sampling time interval is Δ , starting from a certain moment t_1 , at n moments $[t_1, t_2, t_3, t_4, \dots, t_N]$, and sampling to obtain n instantaneous values of short-circuit current $[i_{s1}, i_{s2}, i_{s3}, i_{s4}, \dots, i_{sN}]$, then

$$t_j = t_1 + (j-1)\Delta; \quad t_j + t_d = t_1 + t_d + (j-1)\Delta; \quad t_j - t_d = t_1 - t_d + (j-1)\Delta \quad (5)$$

In Equation (5), j is number of sampling points, $j = 1, 2, 3, \dots, n$. Constructing a function:

$$F = \sum_{j=1}^N (i_{sj} - i_s(t_j))^2 \quad (6)$$

Then, the process of obtaining $X_1, X_2, X_3,$ and X_4 is the process of obtaining the appropriate values of $X_1, X_2, X_3,$ and X_4 to make the function F obtain the minimum value. The F derivative of $X_1, X_2, X_3,$ and $X_4,$ respectively, is such that

$$\begin{cases} \frac{\partial F}{\partial X_1} = -2 \sum_{j=1}^N (i_{sj} - i_s(t_j))k_s(t_j) \\ \frac{\partial F}{\partial X_2} = 2 \sum_{j=1}^N (i_{sj} - i_s(t_j))k_c(t_j) \\ \frac{\partial F}{\partial X_3} = -2 \sum_{j=1}^N (i_{sj} - i_s(t_j)) \\ \frac{\partial F}{\partial X_4} = -2 \sum_{j=1}^N (i_{sj} - i_s(t_j))\Delta(t_j) \end{cases} \tag{7}$$

Letting $\frac{dF}{dt_{bm}} = 0$ and $\frac{dF}{da} = 0,$ a pair of joint cubic equations can be obtained. Joint cubic equations system:

$$\begin{cases} \sum_{j=1}^N (i_{sj} - i_s(t_j))k_s(t_j) = 0 \\ \sum_{j=1}^N (i_{sj} - i_s(t_j))k_c(t_j) = 0 \\ \sum_{j=1}^N (i_{sj} - i_s(t_j)) = 0 \\ \sum_{j=1}^N (i_{sj} - i_s(t_j))\Delta(t_j) = 0 \end{cases} \tag{8}$$

Bringing in the expression for $i_s(t_j)$ yields

$$\begin{cases} X_1 \sum_{j=1}^N k_s^2(t_j) - X_2 \sum_{j=1}^N k_s(t_j)k_c(t_j) + X_3 \sum_{j=1}^N k_s(t_j) - X_4 \sum_{j=1}^N k_s(t_j)\Delta(t_j) = \sum_{j=1}^N k_s(t_j)i_{sj} \\ X_1 \sum_{j=1}^N k_s(t_j)k_c(t_j) - X_2 \sum_{j=1}^N k_c^2(t_j) + X_3 \sum_{j=1}^N k_c(t_j) - X_4 \sum_{j=1}^N k_c(t_j)\Delta(t_j) = \sum_{j=1}^N k_c(t_j)i_{sj} \\ X_1 \sum_{j=1}^N k_s(t_j) - X_2 \sum_{j=1}^N k_c(t_j) + NX_3 - X_4 \sum_{j=1}^N \Delta(t_j) = \sum_{j=1}^N i_{sj} \\ X_1 \sum_{j=1}^N k_s(t_j)\Delta(t_j) - X_2 \sum_{j=1}^N k_c(t_j)\Delta(t_j) + X_3 \sum_{j=1}^N \Delta(t_j) - X_4 \sum_{j=1}^N \Delta^2(t_j) = \sum_{j=1}^N i_{sj}\Delta(t_j) \end{cases} \tag{9}$$

Letting $a = \sum_{j=1}^N k_s^2(t_j), b = \sum_{j=1}^N k_s(t_j)k_c(t_j), c = \sum_{j=1}^N k_s(t_j), d = \sum_{j=1}^N k_s(t_j)\Delta(t_j),$
 $e = \sum_{j=1}^N k_s(t_j)i_{sj}, f = \sum_{j=1}^N k_c^2(t_j), g = \sum_{j=1}^N k_c(t_j), h = \sum_{j=1}^N k_c(t_j)\Delta(t_j), i = \sum_{j=1}^N k_c(t_j)i_{sj},$
 $m = \sum_{j=1}^N \Delta(t_j), p = \sum_{j=1}^N i_{sj}, q = \sum_{j=1}^N \Delta^2(t_j),$ and $r = \sum_{j=1}^N i_{sj}\Delta(t_j),$ the equations above can be rewritten as

$$\begin{cases} aX_1 - bX_2 + cX_3 - dX_4 = e \\ bX_1 - fX_2 + gX_3 - hX_4 = i \\ cX_1 - gX_2 + NX_3 - mX_4 = p \\ dX_1 - hX_2 + mX_3 - qX_4 = r \end{cases} \tag{10}$$

This can be written in matrix form as

$$AX = Y \tag{11}$$

In Equation (11), $A = \begin{bmatrix} a & -b & c & -d \\ b & -f & g & -h \\ c & -g & N & -m \\ d & -h & m & -q \end{bmatrix}$; $X = \begin{bmatrix} X_1 \\ X_2 \\ X_3 \\ X_4 \end{bmatrix}$; $Y = \begin{bmatrix} e \\ i \\ p \\ r \end{bmatrix}$.

The specific calculation formulas of $X_1, X_2, X_3,$ and X_4 are derived in advance, which will minimize the solution calculation time. According to Clem’s rule [29,30] for solving systems of general linear equations, the solution of Equation (11) is

$$\begin{aligned}
 X_1 = \frac{\Delta_1}{\Delta} &= \frac{\begin{vmatrix} e & -b & c & -d \\ i & -f & g & -h \\ p & -g & N & -m \\ r & -h & m & -q \end{vmatrix}}{\begin{vmatrix} a & -b & c & -d \\ b & -f & g & -h \\ c & -g & N & -m \\ d & -h & m & -q \end{vmatrix}}; & X_2 = \frac{\Delta_2}{\Delta} &= \frac{\begin{vmatrix} a & e & c & -d \\ b & i & g & -h \\ c & p & N & -m \\ d & r & m & -q \end{vmatrix}}{\begin{vmatrix} a & -b & c & -d \\ b & -f & g & -h \\ c & -g & N & -m \\ d & -h & m & -q \end{vmatrix}}; \\
 X_3 = \frac{\Delta_3}{\Delta} &= \frac{\begin{vmatrix} a & -b & e & -d \\ b & -f & i & -h \\ c & -g & p & -m \\ d & -h & r & -q \end{vmatrix}}{\begin{vmatrix} a & -b & c & -d \\ b & -f & g & -h \\ c & -g & N & -m \\ d & -h & m & -q \end{vmatrix}}; & X_4 = \frac{\Delta_4}{\Delta} &= \frac{\begin{vmatrix} a & -b & c & e \\ b & -f & g & i \\ c & -g & N & p \\ d & -h & m & r \end{vmatrix}}{\begin{vmatrix} a & -b & c & -d \\ b & -f & g & -h \\ c & -g & N & -m \\ d & -h & m & -q \end{vmatrix}}
 \end{aligned} \tag{12}$$

It can be seen from Equation (12) that simply by finding the values of $a, b, c, d, e, f, g, h, i, m, p, q,$ and $r,$ the values of $X_1, X_2, X_3,$ and X_4 can be found with minimum computation time. The speed of calculation of the coefficients $a, b, c, d, e, f, g, h, i, m, p, q,$ and r has a direct impact on the speed of obtaining the characteristic parameters of the short-circuit current waveform. In the following, the calculation of these coefficients is discussed in the hope that the fastest method of calculation can be obtained.

According to the previous analysis, coefficient a is calculated as:

$$\begin{aligned}
 a &= \sum_{j=1}^N k_s^2(t_j) \\
 &= \sum_{j=1}^N \sin^2(\omega t_j) \\
 &= \sum_{j=1}^N \sin^2(\omega t_1 + \omega(j-1)\Delta) \\
 &= \sin^2(\omega t_1) \sum_{j=1}^N \cos^2(\omega(j-1)\Delta) + \cos^2(\omega t_1) \sum_{j=1}^N \sin^2(\omega(j-1)\Delta) + 0.5 \sin(2\omega t_1) \sum_{j=1}^N \sin(2\omega(j-1)\Delta)
 \end{aligned} \tag{13}$$

In Equation (13), $\sum_{j=1}^N \cos^2(\omega(j-1)\Delta), \sum_{j=1}^N \sin^2(\omega(j-1)\Delta),$ and $\sum_{j=1}^N \sin(2\omega(j-1)\Delta)$ are only related to Δ and $N,$ and they were calculated when the short-circuit current detection system was developed. Letting $\sum_{j=1}^N \cos^2(\omega(j-1)\Delta) = K_1, \sum_{j=1}^N \sin^2(\omega(j-1)\Delta) = K_2,$

$\sum_{j=1}^N \sin(2\omega(j-1)\Delta) = K_3, a$ is simplified as

$$a = K_1 \sin^2(\omega t_1) + K_2 \cos^2(\omega t_1) + 0.5K_3 \sin(2\omega t_1) \tag{14}$$

As can be seen, a is quickly calculated once the detection start time t_1 has been determined.

Similarly, the other parameters can be quickly calculated as follows:

$$\begin{cases} b = 0.5K_4 \sin(2\omega t_1) + 0.5K_3 \cos(2\omega t_1) \\ K_4 = \sum_{j=1}^N \cos(2\omega(j-1)\Delta) \end{cases} \quad (15)$$

$$\begin{cases} c = \sum_{j=1}^N k_s(t_j) = K_5 \sin(\omega t_1) + K_6 \cos(\omega t_1) \\ K_5 = \sum_{j=1}^N \cos(\omega(j-1)\Delta) \\ K_6 = \sum_{j=1}^N \sin(\omega(j-1)\Delta) \end{cases} \quad (16)$$

$$\begin{cases} d = K_5(t_1 - t_d) \sin(\omega t_1) + K_6(t_1 - t_d) \cos(\omega t_1) + K_7 \sin(\omega t_1) + K_8 \cos(\omega t_1) \\ K_7 = \sum_{j=1}^N (j-1)\Delta \cos(\omega(j-1)\Delta) \\ K_8 = \sum_{j=1}^N (j-1)\Delta \sin(\omega(j-1)\Delta) \end{cases} \quad (17)$$

$$f = K_1 \cos^2(\omega t_1) + K_2 \sin^2(\omega t_1) - 0.5K_3 \sin(2\omega t_1) \quad (18)$$

$$g = K_5 \cos(\omega t_1) - K_6 \sin(\omega t_1) \quad (19)$$

$$h = K_5(t_1 - t_d) \cos(\omega t_1) - K_6(t_1 - t_d) \sin(\omega t_1) + K_7 \cos(\omega t_1) - K_8 \sin(\omega t_1) \quad (20)$$

$$m = N(t_1 - t_d) + 0.5N(N-1)\Delta \quad (21)$$

$$q = N(t_1 - t_d)^2 + N(N-1)(t_1 - t_d)\Delta + (2N^3 - 3N^2 + N)\Delta^2/6 \quad (22)$$

The other parameters, $e = \sum_{j=1}^N k_s(t_j)i_{sj}$, $i = \sum_{j=1}^N k_c(t_j)i_{sj}$, $p = \sum_{j=1}^N i_{sj}$, and $r = \sum_{j=1}^N i_{sj}\Delta(t_j)$, need to be calculated on-site after the instantaneous value of the short-circuit current has been obtained.

In summary, the values of $a, b, c, d, e, f, g, h, i, m, p, q$, and r are obtained based on Δ , $t_d, i(t_d), t_1, i(t_1), [t_1, t_2, t_3, t_4, \dots, t_N]$, and $[i_{s1}, i_{s2}, i_{s3}, i_{s4}, \dots, i_{sN}]$; X_1, X_2, X_3 , and X_4 are obtained; short-circuit current waveform parameters I_{bm}, φ_1 , and α are obtained; the fitting of the short-circuit current curve is completed.

3.2. Algorithm Validation

The setting of the ideal short-circuit fault signal in Matlab simulation software is

$$i = 40 \sin(100\pi t - \frac{\pi}{2}) - 35 \sin(-\frac{\pi}{2})e^{-22t} \quad (23)$$

The sampling frequency is set to 10 kHz and a short-circuit fault occurs at $t = 0$ s. Accordingly, the current values at the moment of fault occurrence and the instantaneous values of the short-circuit current $[i_{s1}, i_{s2}, i_{s3}, i_{s4}, \dots, i_{sN}]$ corresponding to the n moments $[t_1, t_2, t_3, t_4, \dots, t_N]$ after the fault occurrence are obtained.

From Equation (3), based on the UDW waveform parameter prediction method, there are two expressions in the process of fitting the short-circuit current curve, namely the exponential expression and linear expression. Assuming $n = 10$, the predicted curve (exponential), the predicted curve (linear), and the actual curve are shown in Figure 3. It can be seen from the figure that both the waveform curve predicted by the exponential expression and the linear expression fit the actual waveform curve very well, but the curve fitted using the exponential expression is closer to the actual curve. The reason for this result is that the linearization of the expression leads to a bias in the identification of the time constants.

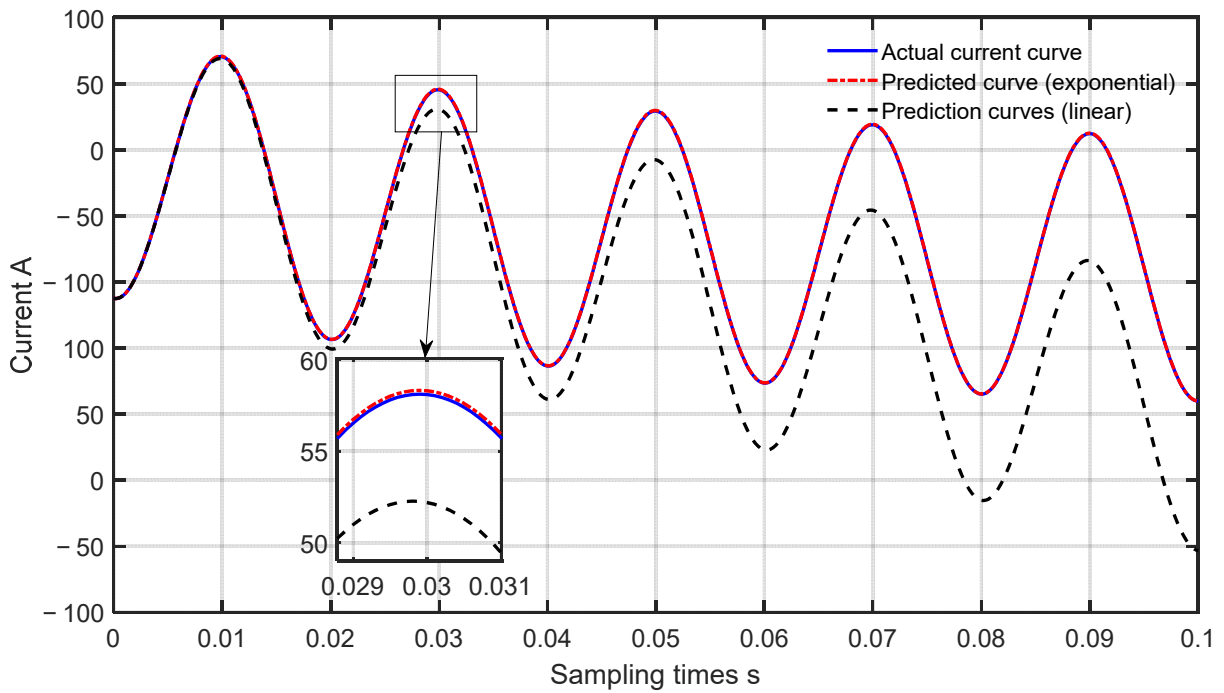


Figure 3. Comparison of predicted and actual curves.

The UDW method is carried out within a very short period of time after the occurrence of a short-circuit, so the value of n cannot be very large. However, if the value of n is too small, the error of curve fitting will be comparatively large. Therefore, the total number of samples n is set to 8–12. As shown in Figure 4 and Table 1, when $n = 10$, the predicted fitted waveform is closest to the predefined waveform, with the lowest errors in I_{bm} , φ_1 , and α . Because the sampling frequency is 10 kHz, the prediction is only 1 ms of the sampling data, which can achieve the purpose of rapid and accurate prediction.

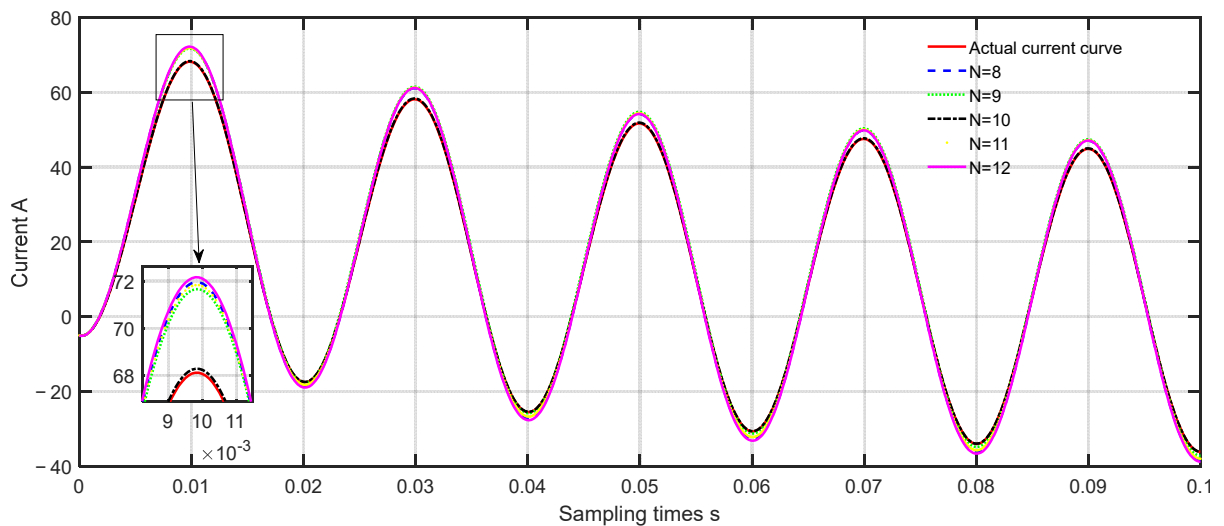


Figure 4. Waveform for different values of n .

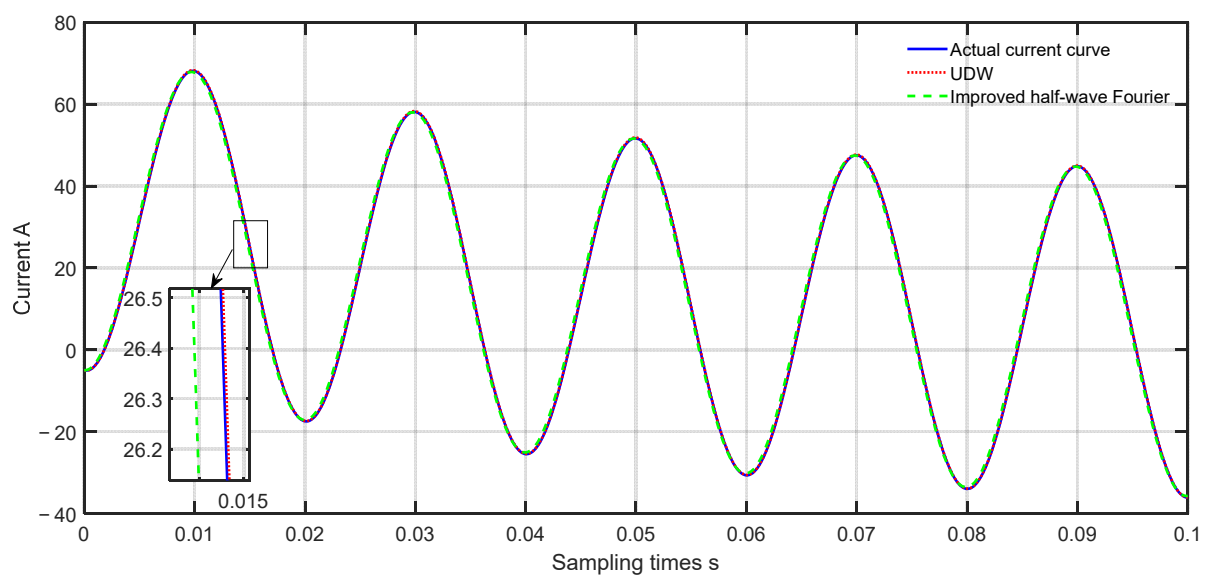
Table 1. Error in waveform parameters when n is taken as different values.

Parameters	Actual Parameters	Error %				
		$n = 8$	$n = 9$	$n = 10$	$n = 11$	$n = 12$
I_{bm}	40 A	5.63	4.40	0.15	5.12	6.07
φ_1	90°	3.09	1.73	0.07	3.44	5.31
α	22	3.45	0.04	0.95	3.72	5.41

In order to further verify the accuracy of this method, the UDW method is compared with the improved half-wave Fourier method [25]. From the comparison of the two waveform prediction methods in Table 2 and Figure 5, it can be seen that the UDW method is the most accurate for the prediction of short-circuit current waveform parameters I_{bm} , φ_1 , and α . Two methods can satisfy the purpose of fast prediction of current parameters, but the improved half-wave Fourier method calculates the steady-state component and transient component separately, which takes longer to calculate than the other.

Table 2. The comparison of the two waveform prediction methods.

Parameters	Error %	
	Improved Half-Wave Fourier	UDW
I_{bm}/A	0.61	0.40
$\varphi_1/^\circ$	2.60	0.07
α	1.98	0.95

**Figure 5.** Comparison of two waveform parameter prediction methods for fitting waveform.

4. Removal of Interference in Short-Circuit Current Signal

In actual work, in the initial stage of the short-circuit current, it is often accompanied by high-frequency interference with high frequency but fast attenuation speed, and there is also noise interference in the actual sampling process [15,16]. Due to the existence of these disturbances, the parameter estimation of the short-circuit current will be larger, biased, or even impossible. For this reason, this paper proposes an interference cancellation method based on trend filtering technology. First, the principles of the trend filtering technique are described. It is then applied to the removal of high-frequency interference and white noise interference, and finally the final conclusions are drawn through simulation.

4.1. Principle of Trend Filtering Technique

It is assumed that for any moment t , the true value of the short-circuit current at that moment is related not only to the 'collected short-circuit current value' at that moment, but also to the 'collected short-circuit current value' at a certain time before and after that moment, and that the true value of the short-circuit current at that moment can be obtained by a weighted average of the above related 'collected short-circuit current value'. The equation is

$$i_k^{(1)} = \frac{\sum_{j=k-m}^{k+m} k_j i_j^{(0)}}{\sum_{j=k-m}^{k+m} k_j} \quad (24)$$

In Equation (24), $i_k^{(1)}$ is the short-circuit current value at the moment of t_k after filtering, $i_j^{(0)}$ is the short-circuit current value at the moment of t_j before filtering, and k_j is the weight. The above equation indicates that the short-circuit current value $i_k^{(1)}$ at the moment of t_k can be calculated by averaging the weights of the sampling value of short-circuit current $i_k^{(1)}$ at the moment of t_k , sampling values of m short-circuit currents $i_{k-m}^{(0)}, i_{k-m-1}^{(0)}, \dots, i_{k-1}^{(0)}$ before the moment of t_k , and sampling values of m short-circuit currents $i_{k+1}^{(0)}, i_{k+2}^{(0)}, \dots, i_{k+m}^{(0)}$ after the moment of t_k .

The distribution of the weights k_j follows the principle of symmetry, i.e., with k_k as the center of symmetry, i.e., $k_{k-1} = k_{k+1}$, $k_{k-2} = k_{k+2}$, $k_{k-m} = k_{k+m}$. The value of k_j can be considered in accordance with the binary principle. Concretizing it:

For the case of $m = 1$:

$$i_k^{(1)} = \frac{\sum_{j=k-1}^{k+1} k_j i_j^{(0)}}{\sum_{j=k-1}^{k+1} k_j} = \frac{i_{k-1}^{(0)} + 2i_k^{(0)} + i_{k+1}^{(0)}}{4} \quad (25)$$

For the case of $m = 2$:

$$i_k^{(1)} = \frac{\sum_{j=k-2}^{k+2} k_j i_j^{(0)}}{\sum_{j=k-2}^{k+2} k_j} = \frac{i_{k-2}^{(0)} + 2i_{k-1}^{(0)} + 4i_k^{(0)} + 2i_{k+1}^{(0)} + i_{k+2}^{(0)}}{10} \quad (26)$$

For the two endpoints of the waveform, special treatment is required. The starting point is $i_1^{(1)} = i_1^{(0)}$ and the finishing point is $i_N^{(1)} = i_N^{(0)}$.

In general, it is difficult to achieve a good filtering effect after one such trend filtering, so multiple iterations of filtering can be carried out: that is, the output quantity of the previous filtering is used as the input quantity for the next filtering, and another filtering is carried out, and so on, until the desired effect is achieved.

4.2. Elimination of High-Frequency Interference and White Noise Interference of Short-Circuit Current

Assuming that the sampling time interval is Δ , starting from a certain moment t_1 , at N moments $[t_1, t_2, t_3, t_4, \dots, t_N]$, N short-circuit current instantaneous values are sampled $[i_{s1}, i_{s2}, i_{s3}, i_{s4}, \dots, i_{sN}]$. The first part of these current values contains high-frequency interference, while the later ones are the real short-circuit current values. This is reflected in the waveform diagram in Figure 6b. From Figure 6c–f, after multiple filters by trend filtering technology, the high-frequency components are almost completely eliminated, and finally, a short-circuit current waveform without high-frequency components is obtained. Moreover, in the part of the original waveform that does not contain high-frequency components, the filtering hardly changes the original waveform. Therefore, it can be considered that the

rapid elimination of high-frequency interference can be achieved by performing multiple trend filtering on only those parts of the original waveform that contain high-frequency components. When using the ultra-short-time data window method to predict the short-circuit current waveform parameters, as there are not much data to be collected, all the collected data can be trend-filtered.

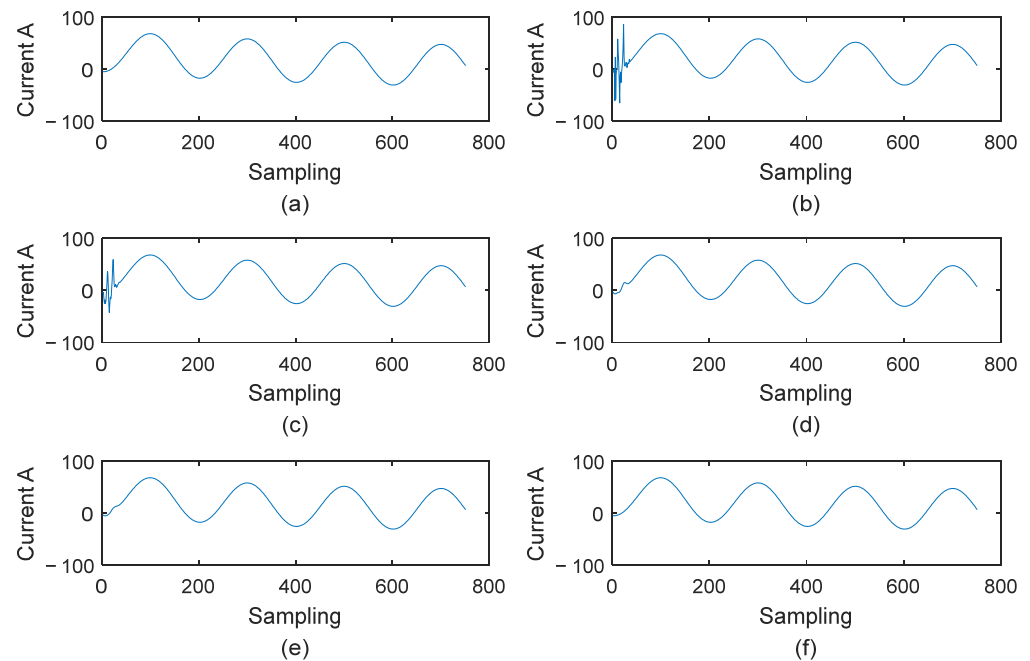


Figure 6. Trend filtering technology eliminates high-frequency interference of short-circuit current. (a) Ideal waveform without any interference. (b) The addition of the high frequency interference to the ideal waveform. (c) One-time filtering effect. (d) Fifteen filtering effect. (e) Thirty filtering effect. (f) Forty-five filtering effect.

There is also the problem of noise interference during the actual sampling. To this end, wgn (White Gaussian Noise) is used to add white noise interference to the original fault current waveform, and the intensity of the noise is set to 20 dB, as shown in Figure 7b. From Figure 7c–f, it can be seen that after the trend filtering technique has been filtered several times, the white noise interference is almost completely eliminated and the filtered waveform is obtained almost identical to the original waveform, so the trend filtering technique is very obvious for eliminating the short-circuit current.

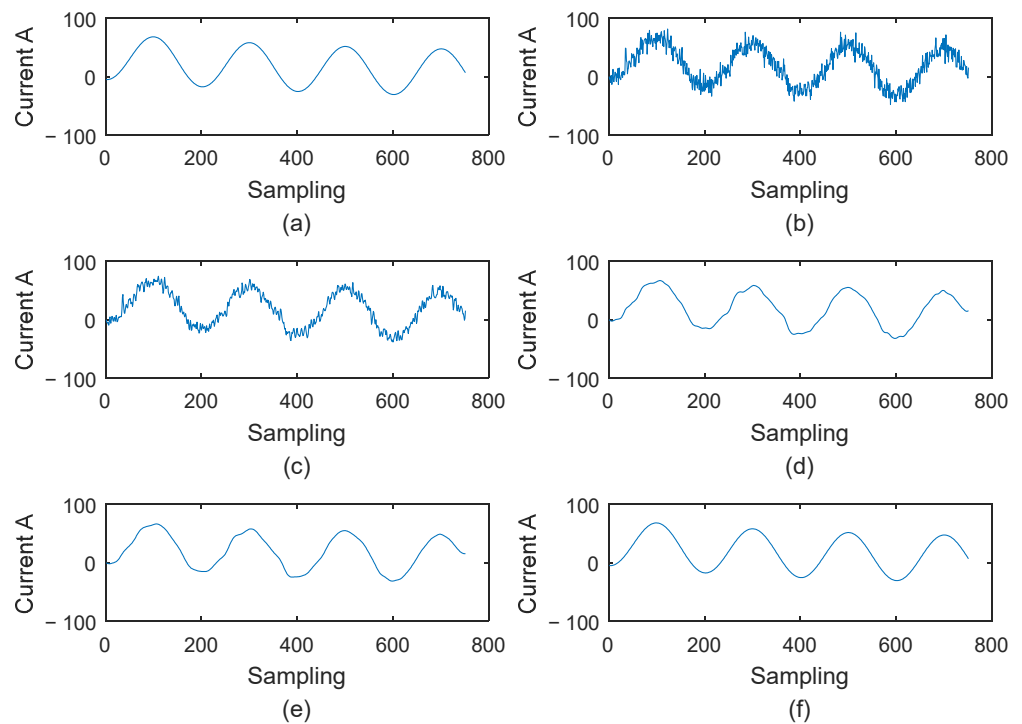


Figure 7. Trend filtering technology eliminates short-circuit current and white noise interference. (a) Ideal waveform without any interference. (b) The addition of the white noise interference to the ideal waveform. (c) One-time filtering effect. (d) Fifteen filtering effect. (e) Thirty filtering effect. (f) Forty-five filtering effect.

5. Measured Short-Circuit Current Waveform

The tests in this paper use a single-phase, small-capacity prototype model to simulate a single-phase short-circuit fault. The experimental circuit diagram is shown in Figure 8. u_s stands for 220 V mains AC. T stands for regulator. K stands for divider controller. R stands for line resistance, and the resistance value is much smaller than the inductance value. L stands for the current limiting inductance value, $L = 12$ mH. The 220 V power supply is turned on, the 120 V voltage is output through the voltage regulator T , the A622 current probe (TEKTRONIX, Beaverton, OR, USA) is used to measure the short-circuit current, the sampling frequency is 10 kHz, and the number of samples required for prediction is set to $N = 10$. The DP05054 oscilloscope (TEKTRONIX, Beaverton, OR, USA) is used to measure and collect the line current waveform in real time, and Matlab software is imported to compare and analyze the test results with the simulation results to further verify the feasibility and accuracy of the UDW prediction short-circuit current parameters proposed in this paper.

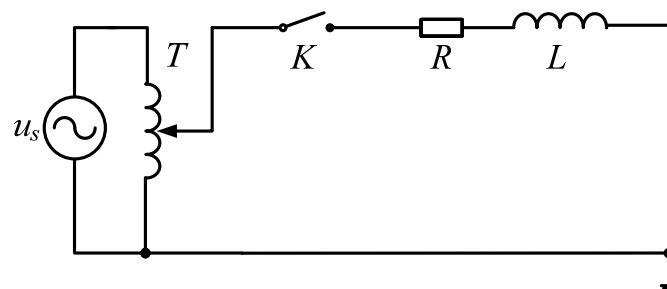


Figure 8. Experimental circuit diagram.

The short-circuit current waveform predicted using the UDW is compared with the measured waveform, from Figure 9a, and the measured short-circuit current waveform is almost the same as the predicted short-circuit current curve. The measured short-circuit current is 54.1255 A. The predicted short-circuit current peak is 51.4164 A, the error is 5%, and the prediction time used is 1 ms. The reason for the large error is because the interference in the signal is too large. The trend filtering technique is used to eliminate disturbances in the short-circuit current, giving a peak-predicted short-circuit current of 53.2205 in Figure 9b, with an error of 1.67%. It can be seen that the short-circuit current predicted by the ultra-short-time data window can quickly and accurately predict the waveform and amplitude of the short-circuit current.

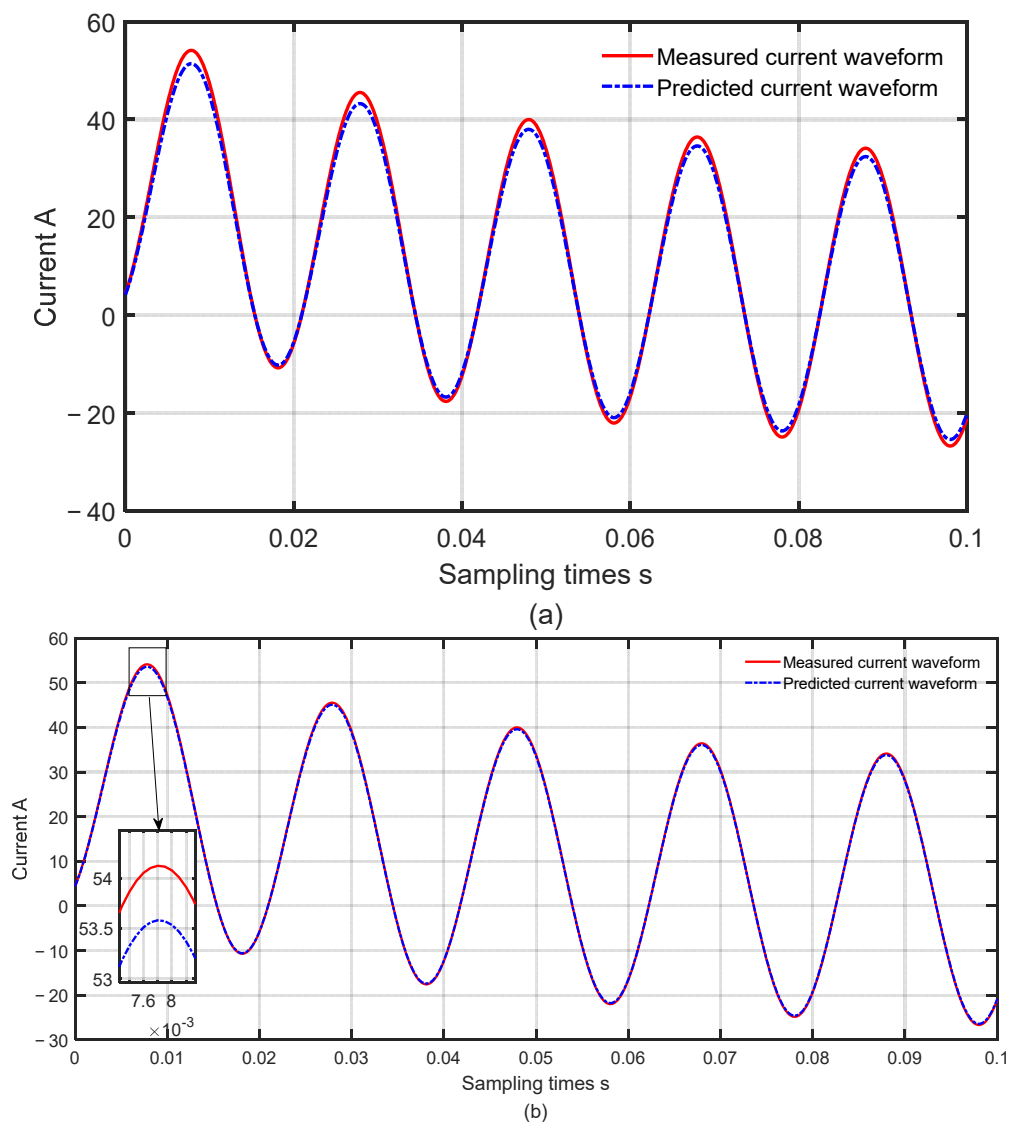


Figure 9. Comparison of measured and predicted waveform. (a) Forecast results without trend filtering technique. (b) Forecast results with trend filtering technique.

6. Conclusions

In this paper, a prediction method based on an ultra-short-time data window is proposed to study the prediction of short-circuit current parameters when a short-circuit failure occurs on a transmission line. Through the analysis of simulation and measured results, the following conclusions are obtained:

- The UDW method has very clear advantages in fitting short-circuit current waveforms to achieve fast and accurate prediction of the waveform parameter. The exponential expressions in the UDW method fit curves closer to the actual curve, with errors of 0.15% for I_{bm} , 0.07% for φ_1 , and 0.95% for α .
- Comparing the UDW method with the modified half-wave Fourier method, it is verified that the UDW method has a shorter prediction time and higher accuracy. The improved half-wave Fourier method has a higher error when the even harmonics increase, whereas the UDW method does not have this problem, so the UDW method is more versatile and has a higher prediction accuracy. The Improved Half-Wave Fourier method calculates the steady-state and transient components separately, which results in a long calculation time, whereas the UDW method requires only 1 ms of sampled data, so the prediction time is shorter.
- Trend filtering technology can realize multiple trend filtering on the sampled data in the initial stage of prediction to achieve the purpose of quickly eliminating high-frequency interference and white noise interference, and improve the accuracy of prediction without affecting the rapidity of prediction.

Author Contributions: Conceptualization, M.W. and X.W.; methodology, M.W., X.W. and Z.Z.; software, M.W.; validation, M.W. and X.W.; formal analysis, M.W., X.W. and Z.Z.; data curation, M.W.; writing—original draft preparation, X.W.; writing—review and editing, M.W., X.W. and Z.Z.; visualization, M.W.; supervision, X.W.; project administration, X.W. All authors have read and agreed to the published version of the manuscript.

Funding: This research was funded by the National Key Research and Development Program of China, grant number 2017YFB0902705.

Institutional Review Board Statement: Not applicable.

Informed Consent Statement: Not applicable.

Data Availability Statement: Not applicable.

Conflicts of Interest: The authors declare no conflict of interest.

References

1. Lou, Y.; Zha, Z.; Li, Z.; Wan, L. Delayed Current Zero Crossing Characteristics for Circuit Breaker Interrupting Short-Circuit Current Following Permanent Single-phase Ground Fault on Short 1000 kV AC Lines. In Proceedings of the 2019 IEEE Asia Power and Energy Engineering Conference (APEEC), Chengdu, China, 29–31 March 2019; pp. 49–54. [\[CrossRef\]](#)
2. Wang, H.; Xu, F.; Jiao, D.; Hu, K.; Yu, L.; Zhang, Y. Analysis on the problems of three-phase short circuit current over-limited of 500 kV bus when UHV connected to Beijing power grid. In Proceedings of the 2016 IEEE PES Asia-Pacific Power and Energy Engineering Conference (APPEEC), Xi'an, China, 25–28 October 2016; pp. 581–585. [\[CrossRef\]](#)
3. Ye, L.; Lin, L.Z.; Juengst, K.-P. Application studies of superconducting fault current limiters in electric power systems. *IEEE Trans. Appl. Supercond.* **2022**, *12*, 900–903. [\[CrossRef\]](#)
4. Chae, W.; Lee, J.H.; Kim, W.H.; Hwang, S.; Kim, J.O.; Kim, J.E. Adaptive Protection Coordination Method Design of Remote Microgrid for Three-Phase Short Circuit Fault. *Energies* **2021**, *14*, 7754. [\[CrossRef\]](#)
5. Zhang, X.H.; Sheng, S.Q.; Li, F.Q.; Hu, Y.O.; Zhang, W.C.; Pan, Y. Analysis of Limiting Measures of Three-phase Short-circuit Current of 500kV Intensive Receiving-end Power Grid in the Early Stage of UHV Construction. *MATEC Web Conf.* **2016**, *63*, 01039. [\[CrossRef\]](#)
6. Chen, H.X.; Jun, W.D.; Shi, H.H. Research on Real-Time Transient Current Carrying of Overhead Transmission Lines. In Proceedings of the 2019 8th International Conference on Advanced Materials and Computer Science (ICAMCS 2019), Chongqing, China, 25–28 December 2019; pp. 367–370. [\[CrossRef\]](#)
7. Zhao, J.Q.; LI, J.; Wu, X.C.; Men, K.; Hong, C. A novel real-time transient stability prediction method based on post-disturbance voltage trajectories. In Proceedings of the 2011 International Conference on Advanced Power System Automation and Protection (APAP 2011), Guangzhou, China, 16 October 2011; pp. 789–795.
8. Ayvaz, A.; Boylu, A.B. Determination of optimal placement of fault current limiting device against short circuit faults occur in power systems. *Sakarya Univ. J. Sci.* **2018**, *22*, 615–623. [\[CrossRef\]](#)
9. Dhara, S.; Shrivastav, A.K.; Sadhu, P.K. A fault current limiter circuit to improve transient stability in power system. *Int. J. Power Electron. Drive Syst.* **2016**, *7*, 769–780. [\[CrossRef\]](#)
10. Yamaguchi, H.; Kataoka, T. Effect of Magnetic Saturation on the Current Limiting Characteristics of Transformer Type Superconducting Fault Current Limiter. *IEEE Trans. Appl. Supercond.* **2006**, *16*, 691–694. [\[CrossRef\]](#)

11. Alam, M.S.; Abido, M.A.Y.; El-Amin, I. Fault Current Limiters in Power Systems: A Comprehensive Review. *Energies* **2018**, *11*, 1025. [[CrossRef](#)]
12. Kheirollahi, R.; Zhao, S.; Lu, F. Fault Current Bypass-Based LVDC Solid-State Circuit Breakers. *IEEE Trans. Power Electr.* **2022**, *37*, 7–13. [[CrossRef](#)]
13. Liu, Y.; Huang, M.; Zha, X. Short-circuit current estimation of modular multilevel converter using discrete-time modeling. *IEEE Trans. Pow. Electr.* **2019**, *34*, 40–45. [[CrossRef](#)]
14. Lee, J.-I.; Dao, V.Q.; Dinh, M.-C.; Lee, S.-j.; Kim, C.S.; Park, M. Combined Operation Analysis of a Saturated Iron-Core Superconducting Fault Current Limiter and Circuit Breaker for an HVDC System Protection. *Energies* **2021**, *14*, 7993. [[CrossRef](#)]
15. Roscoe, A.J.; Blair, S.M.; Dickerson, B.; Rietveld, G. Dealing with Front-End White Noise on Differentiated Measurements Such as Frequency and ROCOF in Power Systems. *IEEE Trans. Instrum. Meas.* **2018**, *67*, 2579–2591. [[CrossRef](#)]
16. Zhang, Y.; Wang, Z.; Zhang, J. Fault detection under strong white Gaussian noise background in power systems. *ICIC Express Lett.* **2011**, *5*, 1473–1479.
17. Chen, J.; Miu, X. Short circuit current peak prediction based on two-dimensional cloud model. *Power Syst. Prot. Control* **2018**, *46*, 94–101. (In Chinese)
18. Wang, M.; Wei, X. Short-circuit current prediction technology based on particle swarm optimization extreme learning machine. *Electr. Mach. Control* **2022**, *26*, 68–76. (In Chinese) [[CrossRef](#)]
19. Chen, L.-a. Prediction for Magnitude of Short Circuit Current in Power Distribution System Based on ANN. Intelligent Information Technology Application Association. In Proceedings of the 2011 International Symposium on Computer Science and Society (ISCCS 2011), Kota Kinabalu, Malaysia, 16 July 2011; pp. 144–147.
20. Tang, L.; Miu, X.; Zhuang, S. Application of PSO-ELM in short-circuit current peak prediction of low voltage system. *J. Fuzhou. Unvi.* **2020**, *48*, 471–478. (In Chinese) [[CrossRef](#)]
21. Miao, X.; Wu, X. Early Detection and prediction for short-circuit current in a multi-level low volta-ge system. *Trans. China Electr. Soci.* **2014**, *29*, 177–183. (In Chinese) [[CrossRef](#)]
22. Peng, H.; Zhu, L.; Mo, W.; Wang, Y.; He, Q.; Wu, X. Zero-crossing Prediction of Short-circuit Current Using Recursive Least Square Algorithm. In Proceedings of the 2020 5th Asia Conference on Power and Electrical Engineering (ACPEE), Chengdu, China, 4–7 June 2020; pp. 1360–1364. [[CrossRef](#)]
23. Chen, Q.; Zhang, G.; Liu, J.; Geng, Y.; Wang, J. Study on fast early detecting and rapid accurate fault parameters estimation method for short-circuit fault. In Proceedings of the 2017 4th International Conference on Electric Power Equipment - Switching Technology (ICEPE-ST), Xi’an, China, 22–25 October 2017; pp. 509–513. [[CrossRef](#)]
24. Cao, J.; Zhao, Y.; Zhang, N.; Wang, W.; Wang, D. A research on zero-cross point forecast method of short circuit current. In Proceedings of the 2017 IEEE 2nd Advanced Information Technology, Electronic and Automation Control Conference (IAEAC), Chongqing, China, 25–26 March 2017; pp. 2385–2389. [[CrossRef](#)]
25. Yuan, Z.; Luo, C.; Fang, C.E.; Chen, S.; He, J. Design of Control System for Controlled Fault Interruption Based on Half-wave Fourier Algorithm. *High Volt. Eng.* **2013**, *39*, 869–875. [[CrossRef](#)]
26. Zhang, H.J.; Wang, S.T.; Li, S.Q. Based on Wavelet Packet Feature Band Extracted Research of The Line Selection in Single-phase Ground Short Circuit. In Proceedings of the 2010 IEEE International Conference on Advanced Management Science VOL.01.Institute of Electrical and Electronics Engineers (IEEE ICAMS 2010), Chengdu, China, 9 July 2010; pp. 190–194.
27. Shuin, V.A.; Dobryagina, O.A.; Shadrikova, T.Y.; Kutumov, Y.D. Protection from Single-Phase Short Circuits to Ground Based on Monitoring the Zero Sequence Capacitance in 6–10 kV Cable Networks. *Power. Technol. Eng.* **2021**, *55*, 126–135. [[CrossRef](#)]
28. Ivanov, I.A.; Lyubarsky, D.R.; Rubtsov, A.A.; Tuzlukova, E.V. An Method for Determining the Amplitude of the Forced Periodic Component of the Transient Short-Circuit Current. *Russ. Electr. Eng.* **2021**, *92*, 529–534. [[CrossRef](#)]
29. Julia, J.; Imme, V.B. Cramer’s rule applied to flexible systems of linear equations. *Electron. J. Linear Algebra* **2012**, *24*, 126–152. [[CrossRef](#)]
30. Kyrchei, I. Analogs of Cramer’s rule for the minimum norm least squares solutions of some matrix equations. *Appl. Math. Comput.* **2012**, *218*, 6375–6384. [[CrossRef](#)]